Experimental Gas Hydrate Dissociation Pressures for Pure Methane in Aqueous Solutions of $MgCl_2$ and $CaCl_2$ and for a (Methane + Ethane) Gas Mixture in an Aqueous Solution of (NaCl + $MgCl_2$)

Zadjia Atik,[†] Christoph Windmeier, and Lothar R. Oellrich*

Institut für Technische Thermodynamik und Kältetechnik, Universität Karlsruhe (TH), 76128 Karlsruhe, Germany

Gas hydrate dissociation pressures along the hydrate−liquid−gas equilibrium line in the temperature range (273 to 292) K and for pressures up to 23 MPa have been determined for methane in aqueous unsaturated magnesium chloride solutions w = (1, 5, 10, and 15) % of $MgCl_2$, in a calcium chloride solution w = 17.05 % of $CaCl_2$, and for a (methane + ethane) mixture in an aqueous solution of sodium chloride and magnesium chloride w(NaCl) = 5 % + w($MgCl_2$) = 6.09 % applying an isochoric method. For the methane system, it is shown that considerable deviation from "ideal" behavior occurs at high $MgCl_2$ concentrations. A gas hydrate calculation model has been applied being able to reproduce the experimental dissociation pressures to within ± 2 % as well as efficiently predicting the dissociation pressures and the inhibiting effects of various other electrolyte solutions for gas hydrate systems with pure gases and gas mixtures.

Introduction

Gas hydrates, or more precisely clathrate hydrates, are solid solutions of a volatile solute in a crystalline host lattice made up of water molecules that form a cage-like structure via hydrogen bonds. The cavities can be occupied by gases whose molecular diameters are smaller than the cage diameters with each cavity structure containing one guest molecule (exceptions being hydrates formed at extreme pressures). Among many substances, the major natural gas constituents are well-known to be gas hydrate formers. When hydrates form or dissociate, only hydrogen bonds are considered as major interactions between neighboring water molecules. Generally gas hydrates are known to form three different crystal structures (I, II,[1,2] and H[3]) out of which natural gas constituents mainly form crystal structures I and II. Natural gas hydrates are typically stable for temperatures above the freezing point of water up to even more than 300 K and to pressures above about 0.6 MPa. However, the stability conditions for gas hydrates strongly depend on gas mixture composition. One cubic meter of natural gas hydrates may contain up to approximately 180 m^3 (V_N) gas being about the same amount of gas as in 1 m^3 compressed to about 15 MPa at ambient temperature but less than liquefied natural gas (LNG) at its normal boiling point (about $V_N \approx 600$ m^3). Natural gas is thought to be the premium fuel for the present century as it burns with fewer pollution problems and higher energetic efficiency than other fossil fuels. At sufficiently low temperatures and high pressures, as found beneath the ocean and in permafrost regions, methane (the major component of natural gas) can form gas hydrates and thus offers an enormous potential energy reservoir.[4,5] Among any water-soluble substance, electrolytes act as gas hydrate inhibitors as their presence shifts the equilibrium line at constant pressure to lower temperatures in analogy to the colligative freezing point depression. To correctly estimate the formation conditions of methane gas hydrates in the presence of electrolytes (for instance, deep sea conditions), the exact knowledge of the influence of individual electrolytes is a prerequisite. The influence of the salts NaCl, $CaCl_2$, KI, and Na_2SO_4 on the location of the pressure−temperature equilibrium line has been investigated recently in our lab by Rock.[6] In the open literature, to the best of our knowledge only one source of experimental data with $MgCl_2$ and methane is available[10] showing a quite large scatter and inconsistency, thus not being suitable for an estimation of model parameters for a computational procedure. To arrive at a sound basis, it was therefore decided to carry out experiments for methane in aqueous solutions at four $MgCl_2$ concentrations.

Different techniques can be used for measuring gas hydrate phase behavior: visual, isobaric, and isochoric methods.[8−11] In the isobaric method, hydrate formation and decomposition are detected by a change in volume at constant pressure during temperature change, whereas a corresponding change in pressure and temperature indicate formation and dissociation in the isochoric method. The two latter methods are fundamentally similar and are considered to be superior to the visual method as they allow an automatic execution of the experiments and a more objective determination of the dissociation end point or hydrate equilibrium point, repectively.[11]

In this work, the isochoric method is used to determine hydrate dissociation pressures of methane in aqueous solutions of magnesium chloride w($MgCl_2$) = (1, 5, 10, and 15) %, calcium chloride w($CaCl_2$) = 17.05 %, and hydrate dissociation pressures of a gas mixture consisting of CH_4 (1) + C_2H_6 (2) with x_1 = 0.96 in a mixed salt solution consisting of w(NaCl) = 5 % and w($MgCl_2$) = 6.09 %. The latter was executed in order to complete Rock's[6] investigation of the influence of bivalent ions on the location of the equilibrium curve. The measurements are carried out at pressures up to 23 MPa.

To give a representation and prediction of the experimental values our own program package "HYdrate CALculation" (HYCAL) was applied.[6,7] Consisting of different models for phase descriptions, HYCAL provides a sound basis for predict-

* Corresponding author. E-mail: oellrich@ttk.uni-karlsruhe.de.
[†] Research guest from the University of Sciences and Technology Houari Boumediene, Crystallography-Thermodynamics Laboratory, Faculty of Chemistry, Algiers, Algeria.

10.1021/je060225a CCC: $30.25
Published on Web 08/16/2006

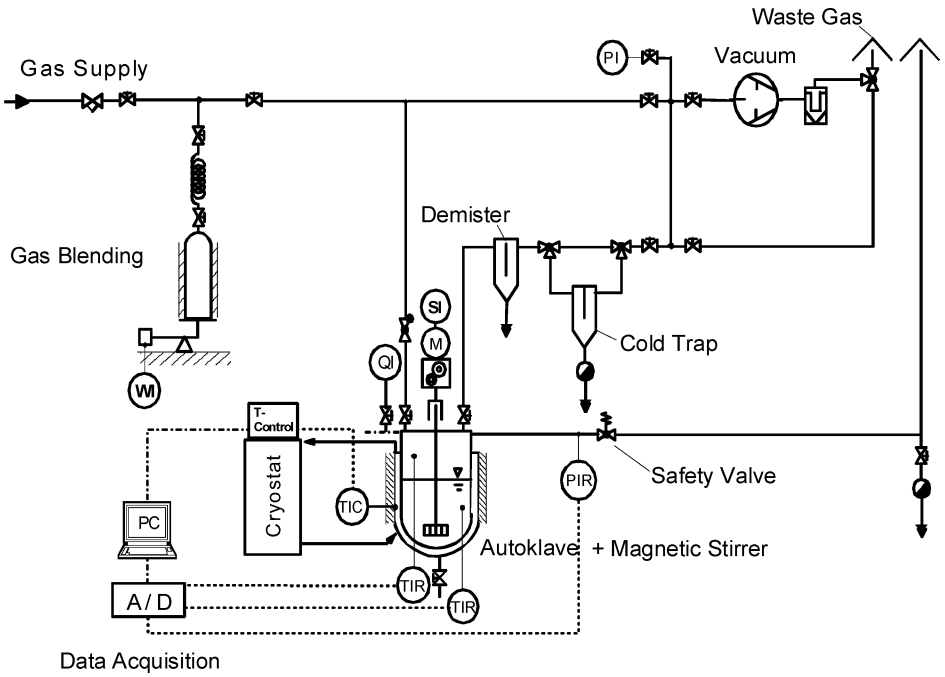

Figure 1. Schematic diagram of the experimental apparatus setup.

ing gas hydrate phase equilibria and accommodates thermodynamically the effect of organic and inorganic inhibitors, pure gases, and gaseous mixtures for pressures up to 25 MPa to a good degree of accuracy. Mean deviations between experimental and calculated pressure values are generally below ± 2 %.

For the description of the solid hydrate phase, an extension of the van der Waals and Platteeuw model[12] is used. For a description of the fluid phases, the Soave−Redlich−Kwong[13] equation of state incorporating the modification by Mathias and Copeman[14,15] and a modified Huron−Vidal G^E mixing rule[16,17] have been implemented. To take into account contributions exerted by electrolytes and organic inhibitors on the molar excess Gibbs free energy G^E as well as on gas solubilities, the LIQUAC approach according to Li and co-workers[18,19] as well as the concept of PSRK[15] are incorporated.

Within the LIQUAC model, G^E is formulated as the sum of contributions from different interaction mechanisms:

$$G^E = G^E_{SR} + G^E_{MR} + G^E_{LR}$$

with G^E_{LR} encompassing the long-range (LR) direct electrostatic interactions between ionic species (taken into account by an extended Debye−Hückel expression), G^E_{MR} is the contribution of medium-range (MR) forces (solvatation effects, a modified Pitzer expression according to Li and co-workers[18,19]), and G^E_{SR} is the short-range (SR) contribution of direct neighboring molecules (represented by a UNIQUAC expression[18,19]). To evaluate the predictive capabilities of our model, the necessary parameters for calculation of water activity were taken directly from literature.

Experimental Section

The methane and the binary gas mixtures (CH_4 (1) + C_2H_6 (2)) with $x_1 = 0.96 \pm 0.0018$ used in this study were supplied by Air Liquide. The pure gases have stated purities of $x = 99.95$ %. The gas purities and mixture composition were confirmed by gas chromatographic analysis. Deionized water (conductivity $\leq 2.0\ \mu S \cdot cm^{-1}$) was used throughout the study. The chemicals were supplied by Carl Roth GmbH with stated purities of $x \geq$ 99.9 % for sodium chloride NaCl, $x \geq 99.5$ % for magnesium chloride $MgCl_2 \cdot 6H_2O$, and $x \geq 99.0$ % for calcium chloride $CaCl_2 \cdot 2H_2O$ on a molar basis. All gases and chemicals were used as received. The water content within the pure salts was considered during preparation of the liquid phase.

Solutions were prepared on a gravimetric basis using a Mettler−Toledo balance (model PR2003 Delta Range) with a precision of $\pm 10^{-3}$ g. A detailed description of the apparatus (the schematic diagram given in Figure 1) and the experimental procedure have been reported elsewhere.[6,7]

The temperature of the constant volume hydrate cell was controlled by a circulation thermostat (JULABO model F32) to within ± 0.05 K and was measured using two Pt-100 thermometers (Philips Thermocoax, Hamburg) that allowed simultaneous temperature readings in the liquid and gaseous phases. The two thermometers were calibrated against a precision Pt-25 thermometer (Rosemount Scientific) according to ITS90. The uncertainty of the measured temperature was within ± 0.02 K corresponding to an error below 0.01 %. The pressure of the hydrate cell is measured using a Rosemount-Pressure Transducer (model 3051TA, 0 to 25 MPa), calibrated against a pressure balance, with a resolution of ± 6 kPa. Including statistical fluctuations, measured pressure values show an overall error below 1 % of the absolute value. Reproducibility of experimental points lies within the stated calibration uncertainties.

For an experiment, the hydrate cell, halfway filled with a degassed aqueous solution and pressurized with a hydrate forming gas (gas mixture, respectively), was readily monitored for a set of measurements by a control and data acquisition computer software (LABVIEW, National Instruments). To enhance gas hydrate formation, optimum stirring of the cell aqueous phase turned out to be about 500 rpm. At first the system was allowed to establish thermal and gas solubility equilibrium outside the hydrate-forming region. The experimental determination of hydrate phase boundaries was initiated by subcooling of at least 10 K below the expected equilibrium point. The stochastic and complicated nature of the nucleation, occurring when cooling the system below the equilibrium

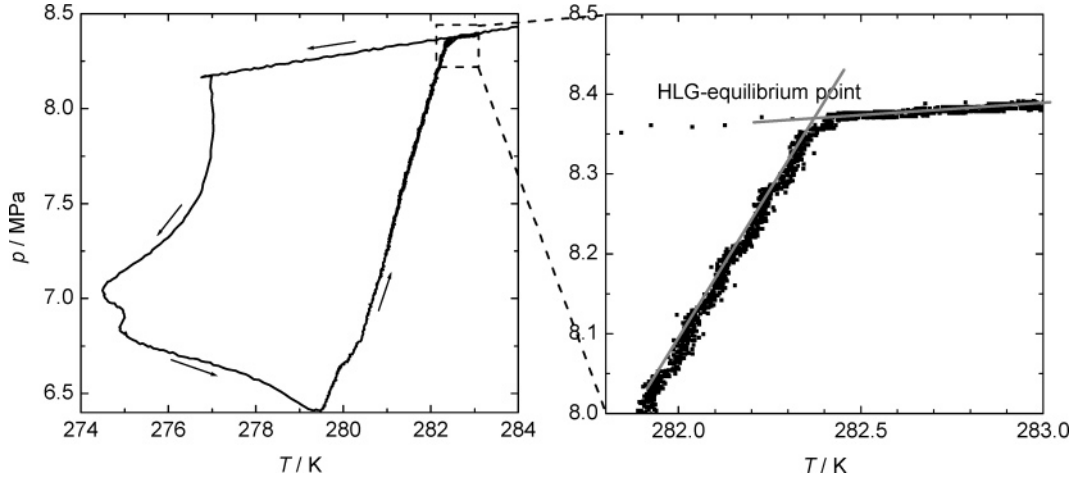

Figure 2. (p, T) trace of methane in an aqueous solution containing $w = 5$ % of $MgCl_2$. Process of hydrate formation and dissociation; determination of equilibrium point.

temperature, depend strongly on the nature and history of the aqueous phase whereas dissociation of the hydrate phase was always thermodynamically reproducible. In this work, the experiment was monitored by the trace of the systems isochoric in the (p, T) plot for observing the formation of the crystalline hydrate phase and finally to determine the hydrate dissociation pressure end point.

Figure 2 exemplifies a (p, T) loop of formation and dissociation of methane hydrate in an aqueous solution of $w(MgCl_2) = 5$ %. To monitor the (p, T) loop efficiently, hydrates were allowed to form corresponding to a pressure decrease of about $\Delta p \approx 2$ MPa. Once formed, the aqueous hydrate suspension was heated progressively back to initial conditions. A discontinuous heating rate resulting in a slow stepwise temperature increase was chosen to be appropriate. Within each step, the hydrate phase was allowed to approach thermodynamic equilibrium using a heating rate ≤ 0.15 K·h^{-1} over a period of about 15 h. At the disappearance of the last hydrate crystals, the dissociation pressure and temperature corresponding to initial liquid and gas-phase compositions were determined by linear regression of two regimes within the (p, T) heating curve. The measured dissociation points were believed to possess an absolute uncertainty below $\pm$ 0.01 % and $\pm$ 1 % for temperature and pressure, respectively (Figure 2). While the aqueous and gas-phase compositions do not stay constant during the formation of hydrates (closed system), the initial compositions of the liquid and gas phases are present only at hydrate dissociation end point values.

Experiments were started at the highest pressure value. Equilibrium points were then obtained by progressive decompression of the hydrate in the system. Due to the objective nature of the experimental procedure, no experiments for reproduction were carried out. The reported data are those of the equilibrium conditions at which the last hydrate crystals dissociate (disappear).

Results and Discussion

The experimental hydrate dissociation pressures in electrolyte solutions are listed in Table 1 for $MgCl_2$ and in Table 2 for $CaCl_2$ for the methane system. They are listed in Table 3 (Figure 5) for the gas mixture. To be able to calculate the corresponding hydrate equilibria using HYCAL, all information except some of the MR and SR interaction parameters of the LIQUAC[18,19] model for the $MgCl_2$ systems were readily available.[18,19] Due to the very low gas solubility and the thus expected very small impact on water activity, the MR and SR values for the $CH_4 + Mg^{2+}$ and the $C_2H_6 + Mg^{2+}$ species combinations were arbitrarily set equal to those of $CH_4 + Ca^{2+}$ and $C_2H_6 + Ca^{2+}$, respectively, and were by these means already available in the literature.[18,19,22] SR $H_2O + Mg^{2+}$ and $Cl^- + Mg^{2+}$ as well as MR $Cl^- + Mg^{2+}$ were taken from refs 18, 19 and 22; a and b parameters for the PSRK equation of state are those of ref 23.

By comparing the predicted data for methane in aqueous solution of $MgCl_2$ with literature values,[10] obtained by a visual method, good agreement of the low concentration literature data is observed. However, all of the previously published data[10] for $w(MgCl_2) = 15$ % are consistently displaced to lower

Table 1. Experimental Dissociation Pressures for Gas Hydrates from Methane in Aqueous $MgCl_2$ Solutions

T/K	p/MPa	T/K	p/MPa
	$w = 1$ %		
292.2	22.65	284.0	8.20
289.0	14.78	280.8	5.83
287.1	11.62		
	$w = 5$ %		
290.0	21.52	282.4	8.37
287.0	14.45	279.9	6.41
284.9	11.11	273.9	3.46
	$w = 10$ %		
285.7	19.42	280.1	9.56
284.4	16.29	276.3	6.24
282.4	12.71		
	$w = 15$ %		
280.2	19.68	273.9	8.71
278.0	14.69	270.4	5.83
276.3	11.72		

Table 2. Experimental Dissociation Pressures for Gas Hydrate from Methane in Aqueous $CaCl_2$ Solution

T/K	p/MPa	T/K	p/MPa
	$w = 17.05$ %		
282.2	22.93	276.3	10.15
280.8	18.63	269.3	4.52
278.7	13.73	265.4	3.03

Table 3. Experimental Dissociation Pressures for Gas Hydrate from a Gas Mixture (CH_4 (1) + C_2H_6 (2)) in an Aqueous Mixed Salt Solution of NaCl and $MgCl_2$

T/K	p/MPa	T/K	p/MPa
	$x_1 = 96$ %, w(NaCl) = 5 %, $w(MgCl_2) = 6.09$ %		
286.0	18.62	283.7	12.32
286.0	18.62	281.7	9.08
285.1	15.78	278.8	6.18

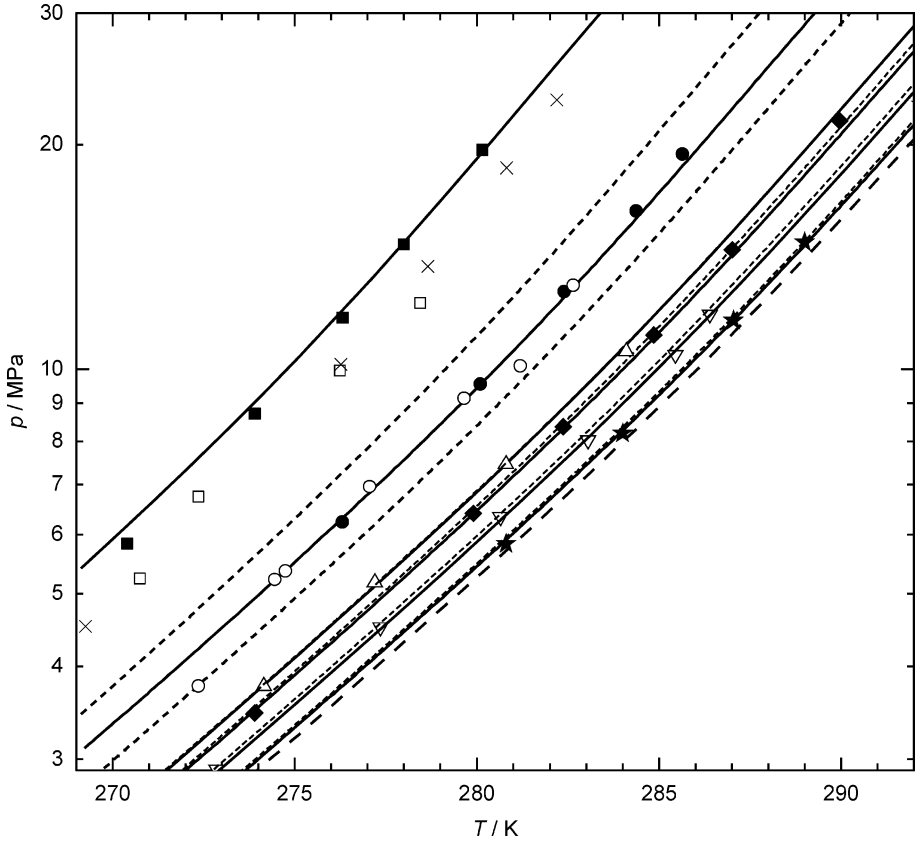

Figure 3. Experimental and predicted hydrate dissociation pressures for the methane gas in solutions of $MgCl_2$ and$CaCl_2$. Solid symbols, this work; open symbols, data from Kang et al.;[10] ■ and □, $w(MgCl_2) = 15$ %; ×, $w(CaCl_2) = 17.05$ %; ● and ○, $w(MgCl_2) = 10$ %; Δ, $w(MgCl_2) = 6$ %; ◆, $w(MgCl_2) = 5$ %; ▽, $w(MgCl_2) = 3$ %; ★, $w(MgCl_2) = 1$ %. Lines: HYCAL[6] predictions (solid); ideal water phase (dotted); pure water (dashed).

pressures as compared to our own experimental data and the predictions (see Figure 3).

Figure 3 shows the effect of the $MgCl_2$ concentration on the hydrate dissociation pressures for the methane system. At low concentrations, experimental as well as calculated values agree practically within experimental uncertainty with the values obtained for a corresponding ideal liquid phase. For this case, the equilibrium point hydrate formation depression can be calculated considering the colligative portion only (water activity coefficient equal to unity) by assuming complete dissociation of the salt. A large increase of the non ideal inhibiting effect of $MgCl_2$ is revealed for the $w(MgCl_2) = 10$ % and, even more pronounced, for the $w(MgCl_2) = 15$ % system. This may indicate a predominant presence of water clustering around ions as well as cation−cation repulsive effects within the water−cation clusters at high salt concentrations, resulting in lower water activity and thus a higher hydrate prevention capability.

For the comparison of the Ca^{2+} and the Mg^{2+} cation, additional experimental data are also included in Figure 3. In both cases, the water mole fraction is equal to 0.903, yielding aqueous solutions of $w(CaCl_2) = 17.05$ % and $w(MgCl_2) = 15$ %, respectively. The comparatively larger influence of Mg^{2+} on the hydrate phase equilibrium can be seen by the larger isobaric shift of equilibrium temperatures toward lower values. As expected, this observation coincides qualitatively with corresponding aqueous freezing point data[24] as shown in Figure 5, which directly correlates to the resulting water activity. In the concentration range considered, $MgCl_2$ causes a larger freezing point depression than $CaCl_2$. Looking at the eutectic behavior of both salts, a shift in inhibition efficiency can be expected around $w(CaCl_2) = 24$ % for calcium chloride, thus making calcium chloride a more efficient inhibitor above this concentration. However, one also has to consider the maximum salt concentration for gas hydrate formation. Berecz and Balla-Achs[25] state this concentration to be around $w(MgCl_2) = 23$ % and $w(CaCl_2) = 26$ %, respectively. It should be noted, however, that these values were obtained by theoretical considerations only and have not yet been verified experimentally. For practical

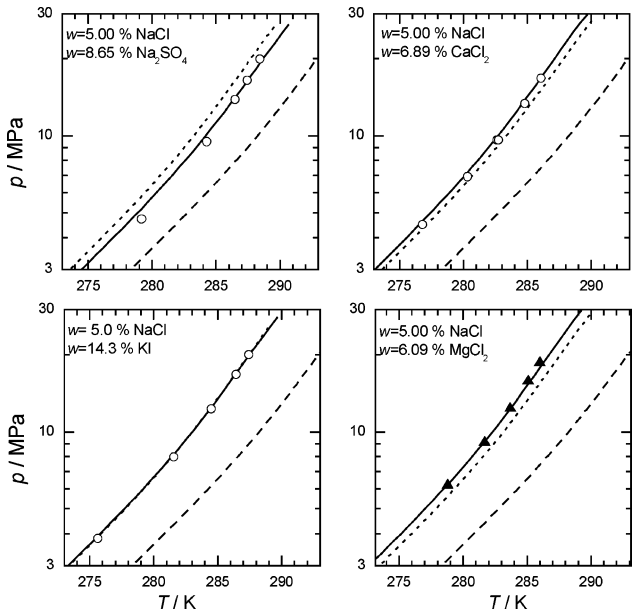

Figure 4. Experimental and predicted hydrate dissociation pressures from a gas mixture (CH_4 (1) + C_2H_6 (2), $x_1 = 0.96$) in various electrolyte solutions having equal ion molar fractions: ▲, this work; ○, Rock.[6] Lines: HYCAL predictions (solid), ideal water phase (dotted), pure water (dashed).

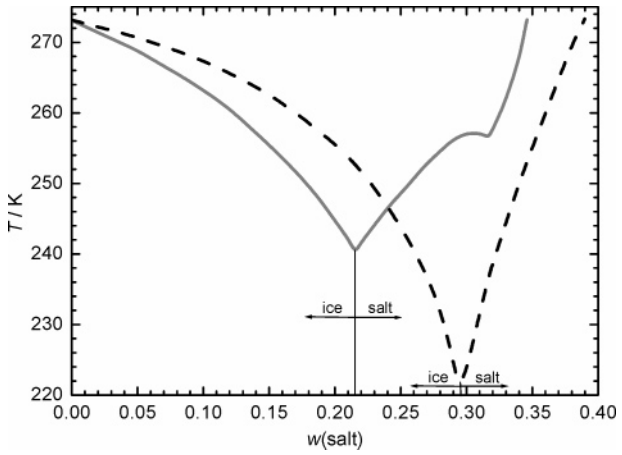

Figure 5. Solid−liquid phase behavior[24] of the systems water + $MgCl_2$ (solid line) and water + $CaCl_2$ (dashed line).

purposes/applications, we conclude that $MgCl_2$ possesses a higher gas hydrate inhibition capability than $CaCl_2$.

The mixed electrolyte experiments ($w(MgCl_2) = 6.09\ \% + w(NaCl) = 5\ \%$) using a binary gas mixture consisting of CH_4 (1) + C_2H_6 (2) with $x_1 = 0.96$ forming hydrate structure II were also carried out in order to complete conclusions drawn in earlier works.[6] The experimental results are shown in Table 3 and together with the HYCAL predictions are plotted in Figure 4 including the earlier experimental results of three other binary electrolyte solutions containing equal NaCl and water molar fractions. In the following, all inhibiting effects will be discussed with respect to the equilibrium line of the ideal mixture ($\gamma_W = 1$) being identical for all four systems. In Figure 4, for the compositions chosen, one again can see the slightly superior inhibition capabilities of NaCl + $MgCl_2$ as compared to the NaCl + $CaCl_2$ system by revealing a larger shift of the equilibrium line toward lower temperatures. As suggested in the above section, this effect is caused by the stronger hydration of the smaller Mg^{2+} ion (higher surface charge density) resulting into a more structured local arrangement of water molecules, thus decreasing the overall water activity. Taking a closer look at all of the electrolyte systems presented, it can be seen that the monovalent NaCl + KI mixture does not seem to show any deviation from ideal behavior (at least at the concentration under consideration) whereas the bivalent NaCl + Na_2SO_4, NaCl + $MgCl_2$, and NaCl + $CaCl_2$ systems significantly deviate from ideal behavior. For the NaCl + $NaSO_4$ system, a positive shift of equilibrium temperatures is noticeable. This effect can be attributed to the fact that anions show a significantly inferior hydration behavior than cations.[26] For the sulfate ion (also being relatively large compared to chloride and iodide), a local weakening of hydrogen bonds for the surrounding water molecules is caused, resulting in a higher water activity and thus in the higher equilibrium temperatures observed.

As a summary, the present data illustrate visible differences in gas hydrate formation conditions due to differences in the ion hydration phenomenon for ions of different size and charge. The degree of ion hydration increases for decreasing ion size and increasing charge. Cations are generally hydrated to a higher degree than anions due to the local charge distribution within the water molecules.[26] Water molecules tend to form hydration shells around charged species whereas larger ions are hydrated to a smaller degree. The phenomenon of ion hydration decreases the amount of free water otherwise available for gas hydrate formation and thus additionally alters resulting water activity.

Conclusions

New data of (H−L−G) conditions for methane and aqueous solution of $MgCl_2$ and $CaCl_2$ as well as for a (methane + ethane) gas mixture in an aqueous solution of (NaCl + $MgCl_2$) have been measured by the isochoric method. A quantitative understanding of the influence on hydrate dissociation pressures in electrolyte solutions is attempted using a thermodynamic hydrate model HYCAL. A larger gas hydrate inhibition capability is shown for $MgCl_2$, with Mg^{2+} being hydrated to a larger degree than Ca^{2+}. This effect can be expected to be prevalent up to the maximum possible concentration for hydrate formation. The effects of ion charge and size on the gas hydrate equilibrium can be traced back to well-known mechanisms of aqueous ion hydration behavior.[26]

Acknowledgment

Z.A. warmly thanks L.R.O. for the invitation, scientific guidance, and excellent research facilities provided for this work and thanks C.W. for continuous scientific and technical assistance.

Literature Cited

(1) von Stackelberg, M. Solid gas hydrates. *Naturwissenschaften* **1949**, *36*, 327−359.
(2) von Stackelberg, M.; Müller, H. R. Solid gas hydrates II. *Z. Elektrochem.* **1954**, *58*, 25−39.
(3) Ripmeester, J. A.; Tse, J. A.; Ratcliffe, C. I., Powell, B. M. A new clathrate hydrate structure. *Nature* **1987**, *325*, 135−136.
(4) Nixdorf, J.; Oellrich, L. R. Natural gas hydrates−from bane to boon? *Nat. Resour. Dev.* **1998**, *47*, 83−98.
(5) Oellrich, L. R. Natural gas hydrates and their potential for future energy supply. *Proceedings of the 6th ISHMT/ASME Heat and Mass Transfer Conference*, January 5−7, 2004, Kalpakkam, India; Proc. HMT-2004-K9; pp 70−78.
(6) Rock, A. M. Experimentelle und theoretische Untersuchung zur Hydratbildung aus Gasgemischen in inhibitorhaltigen wässrigen Lösungen. Dissertation, University Karlsruhe (TH), 2002.
(7) Rock, A. M.; Oellrich, L. R. Hydrate equilibria in aqueous solutions containing inhibitors. *Deutsche Forschungs Gemeinschaft: Properties of Complex Fluid Mixtures*; Research Report; 2004; pp 290−320.
(8) Ross, M. J.; Toczylkin, L. S. Hydrate dissociation pressures for methane or ethane in the presence of aqueous solutions of triethylene glycol. *J. Chem. Eng. Data* **1992**, *37*, 488−491.
(9) de Roo, J. L.; Peters, C. J., Lichtenthaler, R. N.; Diepen, G. A. M. Occurrence of methane hydrate in saturated and unsaturated solutions of sodium chloride and water in dependence of temperature and pressure. *AIChE J.* **1983**, *29* (4), 651−657.
(10) Kang, S.-P.; Chun, M. K.; Lee, H. Phase equilibria of methane and carbon dioxide hydrates in the aqueous $MgCl_2$ solutions. *Fluid Phase Equil.* **1998**, *14* (1−2), 229−238.
(11) Nixdorf, J.; Oellrich, L. R. Experimental determination of hydrate equilibrium conditions for pure, binary and ternary mixtures and natural gases. *Fluid Phase Equilib.* **1997**, *139* (1−2), 325−333.
(12) van der Waals, J. H.; Plateeuw, J. C. *Clathrate Solutions. Advances in Chemical Physics, Vol. II*; Interscience Publishers Inc.: New York, 1959; pp 1−57.
(13) Soave, G. Equilibrium constants from a modified Redlich−Kwong equation of state. *Chem. Eng. Sci.* **1972**, *27* (6), 1197−203.
(14) Mathias, P. M.; Copeman, T. W. Extension of the Peng−Robinson equation of state to complex fluid mixtures: evaluation of the various forms of the local composition concept. *Fluid Phase Equilib.* **1983**, *13*, 91−108.
(15) Holderbaum, T. Die Vorausberechnung von Dampf-Flüssig-Gleichgewichten mit einer Gruppenbeitragszustandsgleichung. Dissertation, University Oldenburg, 1991.
(16) Huron, M. J.; Vidal, J. New mixing rules in simple equations of state for representing vapor−liquid equilibria of strongly non-ideal mixtures. *Fluid Phase Equilib.* **1979**, *3*, 255−271.
(17) Michelsen, M. L. A modified Huron−Vidal mixing rule for cubic equations of state. *Fluid Phase Equilib.* **1990**, *60*, 213-219.
(18) Li, J.; Polka, H. M.; Gmehling, J. A g^E model for single and mixed solvent electrolyte systems. 1. Model and results for strong electrolytes. *Fluid Phase Equilib.* **1994**, *94*, 89−114.
(19) Polka, H.-M.; Li, J.; Gmehling, J. A g^E model for single and mixed solvent electrolyte systems. 2. Results and comparison with other models. *Fluid Phase Equilib.* **1994**, *94*, 115−127.

(20) Sloan Jr., E. D. *Clathrate Hydrate of Natural Gases*, 2nd ed.; Marcel Dekker Inc.: New York, 1998.
(21) Nixdorf, J. Experimentelle und theoretische Untersuchung der Hydratbildung von Erdgasen unter Betriebsbedingungen. Dissertation, Universität Karlsruhe (TH), 1996.
(22) Li, J.; Tophoff, M.; Gmehling, J. Prediction of gas solubilities in aqueous electrolyte systems using the predictive Soave−Redlich−Kwong model. *Ind. Eng. Chem. Res.* **2001**, *40*, 3703−3710.
(23) Harvey, A. H.; Prausnitz, J. M. Thermodynamics of high-pressure aqueous systems containing gases and salts. *AIChE J.* **1989**, *35*, 635−644.
(24) *VDI Wärmeatlas*, 9th ed.; Springer-Verlag: Berlin, 2002.
(25) Berecz, E.; Balla-Achs, M. *Studies in Inorganic Chemistry 4*: *Gas Hydrates*; Elsevier Science Publishers: Amsterdam, The Netherlands, 1983.
(26) Dill, K. A.; Truskett, T..M.; Vojko, V., Hribar-Lee, B. Modelling water, the hydrophobic effect, and ion solvation. *Annu. Rev. Biophys. Struct.* **2005**, *34*, 173−199.

Received for review May 22, 2006. Accepted July 16, 2006. Grateful thanks are due to the DAAD for financial support of this project.

JE060225A